Smart Structures and Systems, *Vol. 25, No. 5* (*2020*) *619-630*
DOI: https://doi.org/10.12989/sss.2020.25.5.619

Nonlinear vibration of smart nonlocal magneto-electro-elastic beams resting on nonlinear elastic substrate with geometrical imperfection and various piezoelectric effects

Laith A. Hassan Kunbar, Luay Badr Hamad, Ridha A. Ahmed and Nadhim M. Faleh*

Al-Mustansiriah University, *Engineering Collage*, *P.O. Box 46049*, *Bab-Muadum*, *Baghdad 10001*, *Iraq*

(*Received September 6, 2019, Revised November 14, 2019, Accepted December 1, 2019*)

Abstract. This paper studies nonlinear free vibration characteristics of nonlocal magneto-electro-elastic (MEE) nanobeams resting on nonlinear elastic substrate having geometrical imperfection by considering piezoelectric reinforcement scheme. The piezoelectric reinforcement can cause an enhanced vibration behavior of smart nanobeams under magnetic field. All of previously reported studies on MEE nanobeams ignore the influences of geometric imperfections which are very substantial due to the reason that a nanobeam cannot be always perfect. Nonlinear governing equations of a smart nanobeam are derived based on classical beam theory and an analytical trend is provided to obtained nonlinear vibration frequency. This research shows that changing the volume fraction of piezoelectric constituent in the material has a great influence on vibration behavior of smart nanobeam under electric and magnetic fields. Also, it can be seen that nonlinear vibration behaviors of smart nanobeam are dependent on the magnitude of exerted electric voltage, magnetic potential, hardening elastic foundation and geometrical imperfection.

Keywords: piezo-magnetic nanobeam; geometrical imperfection; free vibration; piezoelectric reinforcement

1. Introduction

Among different types of smart materials, the multi phases one known as magneto-electro-elastic (MEE) material represents superb possible application in smart structures/systems and also nano-sized devices owning to giving wonderful mechanical, electrical and magnetic coupling performances (Ebrahimi and Barati 2017). Applying electro-magnetic fields to MEE nano-dimension beams yields elastic deformations and changed vibrational properties. Due to the reason that performing experiment on MEE nano-dimension beams are effortful yet, many scholars have represented their theoretical models taking into account small scales influences (Shafiei and She 2018, She *et al*. 2019a, b, Alizada and Sofiyev 2011). Employing nonlocal theory of elasticity (Eringen 1972), one may be able to incorporate the small scales influences in theoretical model of nano-dimension beams (Thai and Vo 2012, Eltaher *et al*. 2012, Zemri *et al*. 2015, Berrabah *et al*. 2013, Bounouara *et al*. 2016, Eltaher *et al*. 2016, Bouafia *et al*. 2017a, b, Mouffoki *et al*. 2017, Yazid *et al*. 2018, Mokhtar *et al*. 2018, Besseghier *et al*. 2017, Ahmed *et al*. 2019). The theory recommends a scale factor called nonlocal parameter for describing that the stress fields at nano scales have a nonlocal character (Barati and Zenkour 2017a, b).

Up to now, several articles have been published about vibrational study of MEE nanoscale beams based on nonlocal theory of elasticity and different beam theories. Using nonlocal theory, an investigation of low amplitude free vibrational characteristics of smart nano-size beam made of MEE material has been carried out by Ke and Wang (2014). In a research, Jandaghian and Rahmani (2016) represented linearly type free vibrational study of magneto-electrically loaded nano-size beams embedded on elastic substrates. Providing exact solutions, Ebrahimi and Barati (2017) researched vibrational characteristics of nonlocal MEE nano-size beams having functionally graded material distribution. Moreover, damping effects due to viscoelasticity on vibrational characteristics of nano-scale beams made of magneto-electric material have been researched by Ebrahimi and Barati (2016). Large amplitude vibrations of MEE nano-size beams using a numerical approach have been studied by Ansari *et al*. (2015).

All of afore-mentioned studies just examined perfect or straight MEE nano-size beams neglecting geometric imperfections influences. Assuming straight beam structures results in inaccurate findings owing to the fact that geometric imperfections are obvious during production as well as mounting of a structure (Mohammadi *et al*. 2014, Barati and Zenkour 2017a, b, Li *et al*. 2018, Eshraghi *et al*. 2016). It has been stated that the vibration behaviors of nano-size beams are relied on the amplitude value of geometrical imperfections. According to this discussion, it may be concluded that it is important to incorporate geometric imperfection effects on vibration behaviors of nonlocal MEE nano-scale beams.

The multi phases composite constructed by piezoelectric and piezo-magnetic constituents exhibits magneto-electrical influences which are invisible in single phase piezoelectric and MEE constituents (Nan 1994). Giving topmost

*Corresponding author, Professor,
E-mail: dr.nadhim@uomustansiriyah.edu.iq

ISSN: 1738-1584 (Print), 1738-1991 (Online)

mechanical efficiency under electrical and magnetic fields, a magneto-electro-elastic (MEE) material may be defined as a species of smart material having different application in sensing apparatus, smart systems and structural components (Aboudi 2001, Pan and Han 2005). Exposing to an exterior mechanical loading, a MEE material is capable to render electrical-magnetic field sensing (Li and Shi 2009, Guo *et al*. 2016). Furthermore, under electro-magnetic fields, such material experiences elastic deformations. For example, $BaTiO_3$ and $CoFe_2O_4$ may be composed to each other for creating a composite of MEE materials (Arefi and Zenkour 2016). According to the percentages of the two constituents, it is feasible to define material properties of the composite such as elastic moduli and piezo-magnetic constants. It is shown by other authors that vibration frequency of MEE structures is sensitive to the percentage of piezoelectric phase and hence vibration behavior of MEE can be controlled by varying the material composition (Kumaravel *et al*. 2007, Annigeri *et al*. 2007).

In this paper, analysis of nonlinear vibrational behaviors of multi-phase magneto-electro-elastic (MEE) nano-size beams has been presented considering geometric imperfection effects. Multi-phase MEE material is composed form piezoelectric and piezo-magnetic constituents for which the material properties can be controlled based on the percentages of the constituents. Nonlinear governing equations of MEE nanobeam are derived based on nonlocal elasticity theory together with classic thin beam model and an approximate solution is provided. It will be shown that nonlinear vibrational behaviors of MEE nanobeam in electro-magnetic field depend on the constituent's percentages. Vibration frequency of MEE nanobeam is also affected by nonlocal scale factor, magnetic field intensity and electrical voltage.

2. Magneto-electro-elastic composites with two phases

For two-phase MEE composites, all material chracteristics are associated with the portion (volume fraction) of piezoelectric constituent (V_f). In the present paper, the nanobeam is made of piezo-magnetic $BaTiO_3$-$CoFe_2O_4$ material and Table 1 represents material coefficients. In this material, $BaTiO_3$ is the piezoelectric constituent and then $CoFe_2O_4$ is the piezo-magnetic constituent. Table 1 respectively defines elastic (C_{ij}), piezoelectric (e_{ij}) and piezo-magnetic (q_{ij}) properties. Moreover, k_{ij}, d_{ij} and x_{ij} respectively denote dielectric, magnetic-electric-elastic and magnetic permeability properties.

3. Beams made of multi-phase MEE material

In order to develop nonlinear formulation for nonlinear vibrations of nonlocal beam, well-known classical beam theory has been used in the present paper. Thus, the displacements of beam (u_1, $u_2 = 0$, u_3) may be written based on axial (u) and transverse (w) field variables as

$$u_1(x,y,z,t) = u(x,y,t) - z\frac{\partial w}{\partial x} \tag{1}$$

$$u_3(x,y,z,t) = w(x,y,t) \tag{2}$$

For the classic beam model, the strain field including geometric imperfection deflection (w^*) might be expressed by

$$\varepsilon_{xx} = \frac{\partial u_1}{\partial x} = \frac{\partial u}{\partial x} - z\frac{\partial^2 w}{\partial x^2} + \frac{1}{2}(\frac{\partial w}{\partial x})^2 + \frac{\partial w}{\partial x}\frac{\partial w^*}{\partial x} \tag{3}$$

Considering the fact that MEE nanobeam is under electro-magnetic field with electrical potential (Φ) and

Table 1 Material properties of $BaTiO_3$-$CoFe_2O_4$ composites (Pan and Han 2005)

Property	$V_f = 0$	$V_f = 0.2$	$V_f = 0.4$	$V_f = 0.6$	$V_f = 0.8$
C_{11} (GPa)	286	250	225	200	175
C_{13}	170	145	125	110	100
C_{33}	269.5	240	220	190	170
e_{31} (C/m^2)	0	-2	-3	-3.5	-4
e_{33}	0	4	7	11	14
q_{31} (N/Am)	580	410	300	200	100
q_{33}	700	550	380	260	120
k_{11} $(10^{-9}$ C/Vm)	0.08	0.33	0.8	0.9	1
k_{33}	0.093	2.5	5	7.5	10
d_{11} $(10^{-12}$ Ns/VC)	0	2.8	4.8	6	6.8
d_{33}	0	2000	2750	2500	1500
x_{11} $(10^{-4}$ $Ns^2/C^2)$	-5.9	-3.9	-2.5	-1.5	-0.8
x_{33}	1.57	1.33	1	0.75	0.5
ρ (kg/m^3)	5300	5400	5500	5600	5700

magnetic potential (Υ), one can define the potentials in following forms as functions of electrical voltage (V_E) and magnetic potential intensity (Ω) (Ebrahimi and Barati 2016)

$$\Phi(x,y,z,t) = -\cos(\beta z)\phi(x,y,t) + \frac{2z}{h}V \tag{4}$$

$$\Upsilon(x,y,z,t) = -\cos(\beta z)\gamma(x,y,t) + \frac{2z}{h}\Omega \tag{5}$$

with $\beta = \pi/h$. Calculating the two-dimensional gradient of electro-magnetic potentials gives the electrical field components (E_x, E_z) and magnet field components (H_x, H_z) as follows

$$\begin{aligned} E_x &= -\Phi_{,x} = \cos(\beta z)\frac{\partial \phi}{\partial x}, \\ E_z &= -\Phi_{,z} = -\beta \sin(\beta z)\phi - \frac{2V}{h} \end{aligned} \tag{6}$$

$$\begin{aligned} H_x &= -\Upsilon_{,x} = \cos(\beta z)\frac{\partial \gamma}{\partial x}, \\ H_z &= -\Upsilon_{,z} = -\beta \sin(\beta z)\gamma - \frac{2\Omega}{h} \end{aligned} \tag{7}$$

For a MEE nano-size beam, the governing equations based on classic beam theory and nonlocal stress effects may be expressed by (Ke and Wang 2014)

$$\frac{\partial N_x}{\partial x} = I_0\frac{\partial^2 u}{\partial t^2} - I_1\frac{\partial^3 w}{\partial x \partial t^2} \tag{8}$$

$$\begin{aligned} &\frac{\partial^2 M_x}{\partial x^2} + \frac{\partial}{\partial x}\left(N_x\left[\frac{\partial w}{\partial x} + \frac{\partial w^*}{\partial x}\right]\right) - k_L w + k_P\frac{\partial^2 w}{\partial x^2} \\ &\qquad - k_{NL}w^3 \\ &= I_0\frac{\partial^2 w}{\partial t^2} + I_1\left(\frac{\partial^3 u}{\partial x \partial t^2}\right) - I_2\nabla^2\left(\frac{\partial^2 w}{\partial t^2}\right) \end{aligned} \tag{9}$$

$$\int_{-h/2}^{h/2}\left(\cos(\beta z)\frac{\partial D_x}{\partial x} + \beta \sin(\beta z)D_z\right)dz = 0 \tag{10}$$

$$\int_{-h/2}^{h/2}\left(\cos(\beta z)\frac{\partial B_x}{\partial x} + \beta \sin(\beta z)B_z\right)dz = 0 \tag{11}$$

in which D_i, B_i represent the components for electric and magnetic field displacements; k_L, k_P, K_{NL} are linear, shear and nonlinear layers of elastic substrate (Sofiyev *et al.* 2017). Also, N_x and M_x are in-plane force and bending moment defined as

$$(N_x, M_x) = \int_A (1, z, f)\sigma_x \, dA \tag{12}$$

and also

$$(I_0, I_1, I_2) = \int_{-h/2}^{h/2}(1, z, z^2)\rho \, dz \tag{13}$$

Note that the material is isotropic, then $I_1 = 0$. Also, the boundary conditions are

$$N_x = 0 \quad \text{or} \quad u = 0 \tag{14}$$

$$\frac{\partial M_x}{\partial x} + N_x\left[\frac{\partial w}{\partial x} + \frac{\partial w^*}{\partial x}\right] = 0 \quad \text{or} \quad w = 0 \tag{15}$$

$$\int_{-h/2}^{h/2}\cos(\beta z)D_x dz = 0 \quad \text{or} \quad \phi = 0 \tag{16}$$

$$\int_{-h/2}^{h/2}\cos(\beta z)B_x dz = 0 \ \text{ or } \ \gamma = 0 \tag{17}$$

All ingredients of stress field, electrical field displacement (D_x, D_z) and magnetic induction (B_x, B_z) for a size-dependent beam relevant to nonlocal theory may be written as (Ebrahimi and Barati 2016)

$$(1-(ea)^2\nabla^2)\sigma_{xx} = \tilde{c}_{11}\varepsilon_{xx} - \tilde{e}_{31}E_z - \tilde{q}_{31}H_z \tag{18}$$

$$(1-(ea)^2\nabla^2)D_x = \tilde{e}_{15}\gamma_{xz} + \tilde{k}_{11}E_x + \tilde{d}_{11}H_x \tag{19}$$

$$(1-(ea)^2\nabla^2)D_z = \tilde{e}_{31}\varepsilon_{xx} + \tilde{k}_{33}E_z + \tilde{d}_{33}H_z \tag{20}$$

$$(1-(ea)^2\nabla^2)B_x = \tilde{q}_{15}\gamma_{xz} + \tilde{d}_{11}E_x + \tilde{\chi}_{11}H_x \tag{21}$$

$$(1-(ea)^2\nabla^2)B_z = \tilde{q}_{31}\varepsilon_{xx} + \tilde{d}_{33}E_z + \tilde{\chi}_{33}H_z \tag{22}$$

So that *ea* is nonlocal scale factor; Elastic, piezoelectric and magnetic material characteristics have been respectively marked by C_{ij}, e_{ij} and q_{ij}. For considering plane stress conditions, all material properties are expressed in a new form a follows (Ke and Wang 2014)

$$\begin{aligned} &\tilde{c}_{11} = c_{11} - \frac{c_{13}^2}{c_{33}}, \quad \tilde{c}_{12} = c_{12} - \frac{c_{13}^2}{c_{33}}, \quad \tilde{c}_{66} = c_{66}, \\ &\tilde{e}_{15} = e_{15}, \qquad \tilde{e}_{31} = e_{31} - \frac{c_{13}e_{33}}{c_{33}}, \\ &\tilde{q}_{15} = q_{15}, \qquad \tilde{q}_{31} = q_{31} - \frac{c_{13}q_{33}}{c_{33}}, \\ &\tilde{d}_{11} = \tilde{d}_{11}, \qquad \tilde{d}_{33} = \tilde{d}_{33} + \frac{q_{33}e_{33}}{c_{33}}, \\ &\tilde{k}_{11} = k_{11}, \qquad \tilde{k}_{33} = k_{33} + \frac{e_{33}^2}{c_{33}}, \\ &\tilde{\chi}_{11} = \chi_{11}, \qquad \tilde{\chi}_{33} = \chi_{33} + \frac{q_{33}^2}{c_{33}} \end{aligned} \tag{23}$$

By integration from Eqs. (18)-(22) over the thickness of nano-size beam, the below resultants for the nano-size beam would be derived

$$\begin{aligned} &(1-(ea)^2\nabla^2)N_x \\ &= A_{11}\left(\frac{\partial u}{\partial x} + \frac{1}{2}\left(\frac{\partial w}{\partial x}\right)^2 + \frac{\partial w}{\partial x}\frac{\partial w^*}{\partial x}\right) \\ &\quad -B_{11}\frac{\partial^2 w}{\partial x^2} + A_{31}^e\phi + A_{31}^m\gamma - N_x^E - N_x^H \end{aligned} \tag{24}$$

$$\begin{aligned} &(1-(ea)^2\nabla^2)M_x \\ &= B_{11}\left(\frac{\partial u}{\partial x} + \frac{1}{2}\left(\frac{\partial w}{\partial x}\right)^2 + \frac{\partial w}{\partial x}\frac{\partial w^*}{\partial x}\right) \\ &\quad -D_{11}\frac{\partial^2 w}{\partial x^2} + E_{31}^e\phi + E_{31}^m\gamma - M_x^E - M_x^H \end{aligned} \tag{25}$$

$$\int_{-\frac{h}{2}}^{\frac{h}{2}}(1-(ea)^2\nabla^2)D_x\cos(\beta z)dz = F_{11}^e\frac{\partial\phi}{\partial x}+F_{11}^m\frac{\partial\gamma}{\partial x} \tag{26}$$

$$(1-(ea)^2\nabla^2)\int_{-\frac{h}{2}}^{\frac{h}{2}}D_z\beta\sin(\beta z)dz = A_{31}^e\left(\frac{\partial u}{\partial x}+\frac{1}{2}\left(\frac{\partial w}{\partial x}\right)^2+\frac{\partial w}{\partial x}\frac{\partial w^*}{\partial x}\right) -E_{31}^e\frac{\partial^2 w}{\partial x^2}-F_{33}^e\phi-F_{33}^m\gamma \tag{27}$$

$$\int_{-\frac{h}{2}}^{\frac{h}{2}}(1-(ea)^2\nabla^2)B_x\cos(\beta z)dz = +F_{11}^m\frac{\partial\phi}{\partial x}+X_{11}^m\frac{\partial\gamma}{\partial x} \tag{28}$$

$$\int_{-\frac{h}{2}}^{\frac{h}{2}}(1-(ea)^2\nabla^2)B_z\beta\sin(\beta z)dz = A_{31}^m\left(\frac{\partial u}{\partial x}+\frac{1}{2}\left(\frac{\partial w}{\partial x}\right)^2+\frac{\partial w}{\partial x}\frac{\partial w^*}{\partial x}\right) -E_{31}^m\nabla^2 w-F_{33}^m\phi-X_{33}^m\gamma \tag{29}$$

in which

$$\{A_{11},B_{11},D_{11}\}=\int_{-h/2}^{h/2}\tilde{c}_{11}(1,z,z^2)\,dz \tag{30}$$

$$\{A_{31}^e,E_{31}^e\}=\int_{-h/2}^{h/2}\tilde{e}_{31}\beta\sin(\beta z)\{1,z\}\,dz \tag{31}$$

$$\{A_{31}^m,E_{31}^m\}=\int_{-h/2}^{h/2}\tilde{q}_{31}\beta\sin(\beta z)\{1,z\}\,dz \tag{32}$$

$$\{F_{11}^e,F_{33}^e\}=\int_{-h/2}^{h/2}\left\{\tilde{k}_{11}\cos^2(\beta z),\tilde{k}_{33}\beta^2\sin^2(\beta z)\right\}dz \tag{33}$$

$$\{F_{11}^m,F_{33}^m\}=\int_{-h/2}^{h/2}\left\{\tilde{d}_{11}\cos^2(\beta z),\tilde{d}_{33}\beta^2\sin^2(\beta z)\right\}dz \tag{34}$$

$$\{X_{11}^m,X_{33}^m\}=\int_{-h/2}^{h/2}\{\tilde{\chi}_{11}\cos^2(\beta z),\tilde{\chi}_{33}\beta^2\sin^2(\beta z)\}\,dz \tag{35}$$

Moreover, electric, magnetic and thermal (N^T) fields exerts in-plane loads and moments which exist in Eqs. (24)-(25) as

$$N_x^E=-\int_{-\frac{h}{2}}^{\frac{h}{2}}\tilde{e}_{31}\frac{2V}{h}dz\,,\qquad N_x^H=-\int_{-h/2}^{h/2}\tilde{q}_{31}\frac{2\Omega}{h}dz \tag{36}$$

$$M_x^E=-\int_{-\frac{h}{2}}^{\frac{h}{2}}\tilde{e}_{31}\frac{2V}{h}zdz, \tag{37}$$

$$M_x^H=-\int_{-h/2}^{h/2}\tilde{q}_{31}\frac{2\Omega}{h}zdz \tag{37}$$

The governing equations for a multi-phase nano-scale beam based upon displacement components would be obtained by inserting Eqs. (24)-(29), into Eqs. (8)-(11) as

$$A_{11}\left(\frac{\partial^2 u}{\partial x^2}+\frac{\partial w}{\partial x}\frac{\partial^2 w}{\partial x^2}+\frac{\partial^2 w}{\partial x^2}\frac{\partial w^*}{\partial x}+\frac{\partial w}{\partial x}\frac{\partial^2 w^*}{\partial x^2}\right) -B_{11}\frac{\partial^3 w}{\partial x^3}+A_{31}^e\frac{\partial\phi}{\partial x}+A_{31}^m\frac{\partial\gamma}{\partial x}=0 \tag{38}$$

$$\begin{aligned}&-D_{11}\frac{\partial^4 w}{\partial x^4}+E_{31}^e\left(\frac{\partial^2\phi}{\partial x^2}\right)+E_{31}^m\left(\frac{\partial^2\gamma}{\partial x^2}\right)\\&+(1-(ea)^2\nabla^2)\left(-I_0\frac{\partial^2 w}{\partial t^2}-I_1\left(\frac{\partial^3 u}{\partial x\partial t^2}\right)\right.\\&+I_2\left(\frac{\partial^4 w}{\partial x^2\partial t^2}\right)+\left(A_{11}\left(\frac{\partial u}{\partial x}+\frac{1}{2}\left(\frac{\partial w}{\partial x}\right)^2+\frac{\partial w}{\partial x}\frac{\partial w^*}{\partial x}\right)\right.\\&\left.\left.-B_{11}\frac{\partial^2 w}{\partial x^2}+A_{31}^e\phi+A_{31}^m\gamma-N_x^E-N_x^H\right)\right.\\&\left.-k_L w+k_P\frac{\partial^2 w}{\partial x^2}-k_{NL}w^3\right)\left[\frac{\partial^2 w}{\partial x^2}+\frac{\partial^2 w^*}{\partial x^2}\right]=0\end{aligned} \tag{39}$$

$$A_{31}^e\left(\frac{\partial u}{\partial x}+\frac{1}{2}\left(\frac{\partial w}{\partial x}\right)^2+\frac{\partial w}{\partial x}\frac{\partial w^*}{\partial x}\right)-E_{31}^e\left(\frac{\partial^2 w}{\partial x^2}\right) +F_{11}^e\left(\frac{\partial^2\phi}{\partial x^2}\right)+F_{11}^m\left(\frac{\partial^2\gamma}{\partial x^2}\right)-F_{33}^e\phi-F_{33}^m\gamma=0 \tag{40}$$

$$A_{31}^m\left(\frac{\partial u}{\partial x}+\frac{1}{2}\left(\frac{\partial w}{\partial x}\right)^2+\frac{\partial w}{\partial x}\frac{\partial w^*}{\partial x}\right)-E_{31}^m\left(\frac{\partial^2 w}{\partial x^2}\right) +F_{11}^m\left(\frac{\partial^2\phi}{\partial x^2}\right)+X_{11}^m\left(\frac{\partial^2\gamma}{\partial x^2}\right)-F_{33}^m\phi-X_{33}^m\gamma=0 \tag{41}$$

An important conclusion from Eq. (38) is

$$A_{11}\left(\frac{\partial u}{\partial x}+\frac{1}{2}\left(\frac{\partial w}{\partial x}\right)^2+\frac{\partial w}{\partial x}\frac{\partial w^*}{\partial x}\right) +A_{31}^e\phi+A_{31}^m\gamma-N_x^E-N_x^H=C_1 \tag{42}$$

Then

$$\frac{\partial u}{\partial x}=-\frac{1}{2}\left(\frac{\partial w}{\partial x}\right)^2-\frac{\partial w}{\partial x}\frac{\partial w^*}{\partial x}-\frac{A_{31}^e}{A_{11}}\phi -\frac{A_{31}^m}{A_{11}}\gamma+\frac{N_x^E}{A_{11}}+\frac{N_x^H}{A_{11}}+\frac{C_1}{A_{11}} \tag{43}$$

Now, integrating Eq. (43) yields

$$u=-\frac{1}{2}\int_0^x(\frac{\partial w}{\partial x})^2\,dx-\int_0^x\frac{\partial w}{\partial x}\frac{\partial w^*}{\partial x}dx-\frac{A_{31}^e}{A_{11}}\int_0^x\phi\,dx -\frac{A_{31}^m}{A_{11}}\int_0^x\gamma\,dx+\frac{N_x^E}{A_{11}}\int_0^x dx+\frac{N_x^H}{A_{11}}\int_0^x dx+\frac{C_1}{A_{11}}x+C_2 \tag{44}$$

Next, by considering boundary conditions $u(0) = 0$, $u(L) = 0$ the two constants would be obtained

$$C_2 = 0$$
$$C_1 = \frac{A_{11}}{2L}\int_0^L (\frac{\partial w}{\partial x})^2\,dx + \frac{A_{11}}{L}\int_0^L \frac{\partial w}{\partial x}\frac{\partial w^*}{\partial x}\,dx + \frac{A_{31}^e}{L}\int_0^L \phi\,dx + \frac{A_{31}^m}{L}\int_0^L \gamma\,dx - (N_x^E + N_x^H) \quad (45)$$

The final governing equations for the MEE nano-size beam will be derived after placing Eq. (43) in Eqs. (39)-(41) as

$$-D_{11}\frac{\partial^4 w}{\partial x^4} + E_{31}^e\left(\frac{\partial^2 \phi}{\partial x^2}\right) + E_{31}^m\left(\frac{\partial^2 \gamma}{\partial x^2}\right) + (1-(ea)^2\nabla^2)\left(-I_0\frac{\partial^2 w}{\partial t^2} - I_1\left(\frac{\partial^3 u}{\partial x \partial t^2}\right) + I_2\left(\frac{\partial^4 w}{\partial x^2 \partial t^2}\right) + \left(A_{11}\left(+\frac{1}{2L}\int_0^L (\frac{\partial w}{\partial x})^2\,dx + \frac{1}{L}\int_0^L \frac{\partial w}{\partial x}\frac{\partial w^*}{\partial x}dx\right) - B_{11}\frac{\partial^2 w}{\partial x^2} - N_x^E - N_x^H\right) - k_L w + k_P\frac{\partial^2 w}{\partial x^2} - k_{NL}w^3\right)\left[\frac{\partial^2 w}{\partial x^2} + \frac{\partial^2 w^*}{\partial x^2}\right] = 0 \quad (46)$$

$$A_{31}^e\left(-\frac{A_{31}^e}{A_{11}}\phi - \frac{A_{31}^m}{A_{11}}\gamma + \frac{1}{2L}\int_0^L \left(\frac{\partial w}{\partial x}\right)^2 dx + \frac{1}{L}\int_0^L \frac{\partial w}{\partial x}\frac{\partial w^*}{\partial x}dx\right) - E_{31}^e\left(\frac{\partial^2 w}{\partial x^2}\right) + F_{11}^e\left(\frac{\partial^2 \phi}{\partial x^2}\right) + F_{11}^m\left(\frac{\partial^2 \gamma}{\partial x^2}\right) - F_{33}^e\phi - F_{33}^m\gamma = 0 \quad (47)$$

$$A_{31}^m\left(-\frac{A_{31}^e}{A_{11}}\phi - \frac{A_{31}^m}{A_{11}}\gamma + \frac{1}{2L}\int_0^L \left(\frac{\partial w}{\partial x}\right)^2 dx + \frac{1}{L}\int_0^L \frac{\partial w}{\partial x}\frac{\partial w^*}{\partial x}dx\right) - E_{31}^m\left(\frac{\partial^2 w}{\partial x^2}\right) + F_{11}^m\left(\frac{\partial^2 \phi}{\partial x^2}\right) + X_{11}^m\left(\frac{\partial^2 \gamma}{\partial x^2}\right) - F_{33}^m\phi - X_{33}^m\gamma = 0 \quad (48)$$

4. Method of solution

The governing equation for MEE nano-size beam only contains three displacements which need to be approximated based on following assumption (Ebrahimi and Barati 2016)

$$w = \sum_{i=1}^{\infty} W_m(t)X_i(x) \quad (49)$$

$$\phi = \sum_{i=1}^{\infty} \Phi_m(t)X_i(x) \quad (50)$$

$$\gamma = \sum_{i=1}^{\infty} \Upsilon_m(t)X_i(x) \quad (51)$$

where (W_{bmn} ,Φ_{mn}, γ_{mn}) are the unknown coefficients and the function X_m defines a trial function for considering boundary conditions; $X_i = Sin(i\pi x/L)$ for simply supported conditions at both ends and $X_i = 0.5(1-\cos 2i\pi x/L))$ for clamped-clamped edges.

Then, the imperfection shape is considered as first buckling mode of the nano-size beam as

$$w^* = \sum_{i=1}^{\infty} W^*(t)F_i(x) \quad (52)$$

in which W^* defines the imperfections amplitude and F_i defines the shape functions for imperfections. Placing Eqs. (49)-(52) into Eqs. (46)-(48) gives three equations as

$$\begin{aligned} &K_1^S W_m + G_1 W_m^3 + Q_1 W_m^2 + M\ddot{W}_m + K_1^E\Phi_m \\ &\quad + K_1^H\Upsilon_m + \Psi_1 W^* = 0 \\ &K_2^S W_m + G_2 W_m^2 + K_2^E\Phi_m + K_2^H\Upsilon_m = 0 \\ &K_3^S W_m + G_3 W_m^2 + K_3^E\Phi_m + K_3^H\Upsilon_m = 0 \end{aligned} \quad (53)$$

in which

$$K_1^S = -D_{11}(\Lambda_{40}) - k_w\Lambda_{00} + k_p\Lambda_{20} - (N_x^E + N_x^H)\Lambda_{20} + (ea)^2(N_x^E + N_x^H)\Lambda_{40} + \frac{A_{11}}{L}\Xi_{11}\Gamma_{20}W^{*2} - (ea)^2\frac{A_{11}}{L}\Xi_{11}\Gamma_{40}W^{*2} \quad (54)$$

$$\begin{aligned} G_1 &= \frac{A_{11}}{2L}\Lambda_{11}\Lambda_{20} - (ea)^2\frac{A_{11}}{2L}\Lambda_{11}\Lambda_{40} \\ &\quad -k_{nl}(\Lambda_{0000} - (ea)^2(\Lambda_{1100} + \Lambda_{2000})) \\ Q_1 &= \frac{A_{11}}{2L}\Lambda_{11}\Gamma_{20}W^* - (ea)^2\frac{A_{11}}{2L}\Lambda_{11}\Gamma_{40}W^* \\ &\quad + \frac{A_{11}}{L}\Xi_{11}\Lambda_{20}W^* - (ea)^2\frac{A_{11}}{L}\Xi_{11}\Lambda_{40}W^* \end{aligned} \quad (55)$$

$$K_1^E = E_{31}^e\Lambda_{20} \quad (56)$$

$$K_1^H = E_{31}^m\Lambda_{20} \quad (57)$$

$$K_2^S = -E_{31}^e\Lambda_{20} + \frac{A_{31}^e}{L}\Lambda_0\Xi_{11}W^* \quad (58)$$

$$K_3^S = -E_{31}^m\Lambda_{20} + \frac{A_{31}^m}{L}\Lambda_0\Xi_{11}W^* \quad (59)$$

$$G_2 = \frac{A_{31}^e}{2L}\Lambda_0\Lambda_{11} \quad (60)$$

$$G_3 = \frac{A_{31}^m}{2L}\Lambda_0\Lambda_{11} \quad (61)$$

$$K_2^E = -\frac{(A_{31}^e)^2}{A_{11}}\Lambda_{00} + F_{11}^e\Lambda_{20} - F_{33}^e\Lambda_{00} \quad (62)$$

$$K_2^H = -\frac{A_{31}^e A_{31}^m}{A_{11}}\Lambda_{00} + F_{11}^m\Lambda_{20} - F_{33}^m\Lambda_{00} \quad (63)$$

$$K_3^E = -\frac{A_{31}^e A_{31}^m}{A_{11}}\Lambda_{00} + F_{11}^m\Lambda_{20} - F_{33}^m\Lambda_{00} \quad (64)$$

$$K_3^H = -\frac{(A_{31}^m)^2}{A_{11}}\Lambda_{00} + X_{11}^m\Lambda_{20} - X_{33}^m\Lambda_{00} \quad (65)$$

$$\Psi_1 = -(N_x^E + N_x^H)\Gamma_{20} + (ea)^2(N_x^E + N_x^H)\Gamma_{40} \quad (66)$$

$$M = -I_0\Lambda_{00} + (ea)^2 I_0\Lambda_{20} + I_2\Lambda_{20} - (ea)^2 I_2\Lambda_{40} \quad (67)$$

where

$$\begin{aligned}
\Lambda_{00} &= \int_0^L X_i X_i dx\,, \quad \Lambda_{20} = \int_0^L X_i^{''} X_i dx \\
\Lambda_{40} &= \int_0^L X_i^{''''} X_i dx\,, \quad \Lambda_{11} = \int_0^L X_i^{'} X_i^{'} dx \\
\tilde{\Lambda}_{00} &= \int_0^L (X_i)^4 dx\,, \quad \Xi_{11} = \int_0^L F_i^{'} X_i^{'} dx \\
\Gamma_{20} &= \int_0^L F_i^{''} F_i dx \\
\Gamma_{40} &= \int_0^L F_i^{''''} F_i dx
\end{aligned} \quad (68)$$

By using last two relations of Eq. (53), one may derive the unknowns Φ_m and Υ_m as follows

$$\begin{aligned}
\Phi_m &= Z_1 W_m + Z_2 W_m^2, \\
\Upsilon_m &= Z_3 W_m + Z_4 W_m^2 \\
Z_1 &= -\frac{(K_2^H K_3^S - K_3^H K_2^S)}{K_3^E K_2^H - K_2^E K_3^H} \\
Z_2 &= -\frac{(G_3 K_2^H - G_2 K_3^H)}{K_3^E K_2^H - K_2^E K_3^H} \\
Z_3 &= -\frac{(K_3^E K_2^S - K_2^E K_3^S)}{K_3^E K_2^H - K_2^E K_3^H} \\
Z_4 &= -\frac{+(G_2 K_3^E - G_3 K_2^E)}{K_3^E K_2^H - K_2^E K_3^H}
\end{aligned} \quad (69)$$

Placing Eq. (69) in the first relation of Eq. (53) results in

$$\frac{K^*}{M} W_m + \frac{G_1}{M} W_m^3 + \frac{Z^*}{M} W_m^2 + \ddot{W}_m + \frac{\Psi_1}{M} W^* = 0 \quad (70)$$

where

$$\begin{aligned}
K^* &= K_1^S + K_1^E Z_1 + K_1^H Z_3 \\
Z^* &= K_1^E Z_2 + K_1^H Z_4 + Q_1
\end{aligned} \quad (71)$$

Next, via performing harmonic balance technique (Besseghier *et al*. 2015), one can solve Eq. (70). Assuming that vibrations of a nano-size beam occur in positive and negative directions of *z* axis, Eq. (70) must be rewritten as

$$\frac{K^*}{M} W_m + \frac{G_1}{M} W_m^3 + \frac{Z^*}{M} W_m |W_m| + \ddot{W}_m + \frac{\Psi_1}{M} W^* = 0 \quad (72)$$

It is supposed that an approximate solution may be defined by (Besseghier *et al*. 2015, Li and Hu 2016)

$$W(t) = \widetilde{W}\, cos(\omega t) \quad (73)$$

in which is $\widetilde{W}$ the maximum vibration amplitude. Next, Eq. (73) is placed into Eq. (72) to obtain the below equation

$$\begin{aligned}
&\frac{K^*}{M} \widetilde{W}\, cos(\omega t) + \frac{G_1}{M} \big(\widetilde{W}\, cos(\omega t)\big)^3 \\
&+ \frac{Z^*}{M} \big(\widetilde{W}\, cos(\omega t)\big) \big|\big(\widetilde{W}\, cos(\omega t)\big)\big| \\
&- \widetilde{W}\omega^2\, cos(\omega t) + \frac{\Psi_1}{M} W^* = 0
\end{aligned} \quad (74)$$

Next, the below function definitions may be used for further calculations

$$\begin{aligned}
|cos(\omega t)| &= \frac{4}{\pi}\Big[\frac{1}{2} + \frac{1}{3} cos(2\omega t) - \frac{1}{15} cos(4\omega t) + \ldots.\Big] \\
cos(\omega t)|cos(\omega t)| &= \frac{4}{\pi}\Big[\frac{1}{2} cos(\omega t) + \frac{1}{3} cos(2\omega t)\, cos(\omega t) \\
&\quad - \frac{1}{15} cos(4\omega t)\, cos(\omega t) + \ldots.\Big] \\
&= \frac{8}{3\pi} cos(\omega t)
\end{aligned} \quad (75)$$

By performing some calculations using above relations, Eq. (74) may be expressed as follows

$$\begin{aligned}
&cos(\omega t)\left[\frac{K^*}{M}\widetilde{W} + \frac{3}{4}\frac{G_1}{M}\widetilde{W}^3 + \frac{8\widetilde{W}^2}{3\pi}\frac{Z^*}{M}\right. \\
&\left. - \widetilde{W}\omega^2\, cos(\omega t)\right] = 0
\end{aligned} \quad (76)$$

From above equation, it is easy to express the nonlinear vibration frequency as

$$\omega_{NL} = \sqrt{\frac{K^*}{M} + \frac{3}{4}\frac{G_1}{M}(\widetilde{W})^2 + \frac{8\widetilde{W}}{3\pi}\frac{Z^*}{M}} \quad (77)$$

Also, dimensionless quantities are selected as

$$\begin{aligned}
&K_L = k_L \frac{L^4}{D_{11}}, \quad K_p = k_p \frac{L^2}{D_{11}}, \quad K_{NL} = k_{NL} \frac{L^4}{A_{11}} \\
&\widetilde{\omega} = \omega L^2 \sqrt{\frac{\rho A}{\tilde{c}_{11} I}}, \quad \mu = \frac{ea}{L}
\end{aligned} \quad (78)$$

5. Numerical results and discussions

Discussions on nonlinear vibration behavior of MEE nanobeams having geometrical imperfection have been presented in this chapter. The nanobeam's length has been selected as L = 10 nm. Due to the reason that there is no published study about vibrations of geometrically imperfect MEE nano-size beams, the vibration frequencies have been verified with those for imperfect elastic nano-size beams without piezoelectric and magnetic field effects. Table 2 represents the nonlinear vibrational frequencies of a nano-dimension beam according to diverse values for maximum vibrational amplitude and also imperfection amplitude (W* = 0, 0.1, 0.2, 0.3) comparing to those presented by Li *et al*. (2018). It is obvious that presented result is identically the same as that provided by Li *et al*. (2018). Another investigation is provided in Table 3 to compare the obtained vibrational frequencies of perfect piezo-magnetic nanobeams with the findings presented by Ke and Wang (2014) based on differential quadrature method. In this table, the frequencies are presented for diverse values of nonlocal parameter and a good agreement with previously

Table 2 Validation of nonlinear vibration frequency for perfect/imperfect nanobeams

		W* = 0	W* = 0.1	W* = 0.2	W* = 0.3
$\widetilde{W}$ = 0.2	Li *et al.* (2018)	9.9065	9.9933	10.1276	10.3075
	Present	9.9065	9.9933	10.1276	10.3075
$\widetilde{W}$ = 0.4	Li *et al.* (2018)	10.0166	10.1636	10.3557	10.5904
	Present	10.0166	10.1636	10.3557	10.5904

Table 3 Validation of vibration frequency for a piezo-magnetic nanobeam with various nonlocal parameters (V = 0, Ω = 0)

	μ = 0	μ = 0.1	μ = 0.2	μ = 0.3	μ = 0.4
Ke and Wang (2014)	3.7388	3.5670	3.1658	2.7209	2.3281
Present	3.7392	3.5675	3.1662	2.7212	2.3283

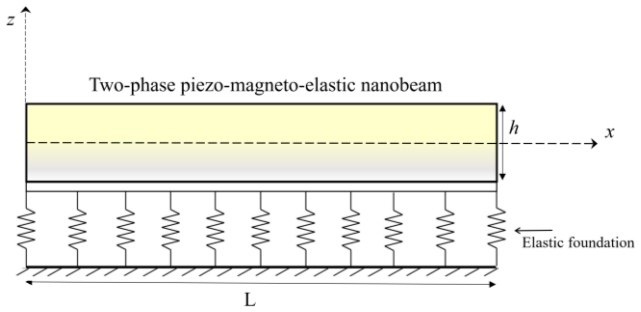

Fig. 1 Configuration of a two-phase smart nanobeam

obtained results is observed.

Fig. 2 illustrates the nonlinear frequency-amplitude curves of a nano-size beam for various nonlocal parameters with and without geometric imperfection effects. In this figure, the piezoelectric phase percentage is set to V_f = 20%; applied electric voltage and magnetic potential are simply considered as V_E = 0, Ω = 0. Simply supported-simply simply supported (S-S) and clamped-clamped (C-C) boundary conditions are considered for the nanobeam. For oscillations in positive ($\widetilde{W}/h > 0$) and negative ($\widetilde{W}/h < 0$) directions, increasing in the magnitude of dimensionless amplitude yields larger vibration frequencies for a perfect nanobeam due to hardening effects raised from geometric nonlinearity. For a perfect nanobeam, the frequency-amplitude curves are symmetric with respect to $\widetilde{W}/h = 0$. However, the frequency-amplitude curves are not symmetric with respect to $\widetilde{W}/h = 0$ for an imperfect nanobeam. In fact, the nonlinear vibration frequency may decrease by increasing in the magnitude of dimensionless amplitude in the region of $\widetilde{W}/h < 0$. For both perfect and imperfect nanobeams, increase of nonlocal parameter yields smaller nonlinear frequencies since the total stiffness of the nanobeam is reduced. So, nonlocal stress field which captures long range atomic interaction has a great influence on vibration characteristics of geometrically imperfect piezo-magnetic nanobeams.

Figs. 3 and 4 respectively show the influences of applied electrical voltages (VE) and magnetic potential (Ω) on nonlinear vibration frequency of a smart nano-scale beam with/without geometric imperfections effects. The piezoelectric constituent volume has been considered as Vf = 20%. One can see that applying negative electrical voltages to a nano-scale beam causes greater nonlinear vibration frequencies than applying a positive electrical voltage. Such observation is because of raised compressive loads by positive electrical voltages. Such compressive loads may result in the decrement in structural stiffness of the nano-scale beam as well as vibration frequency. Another observation is that the effect of magnetic potential on vibration frequency is in contrast to electrical voltages. Actually, negative magnetic potentials yield smaller nonlinear frequency than a positive one. Such observations

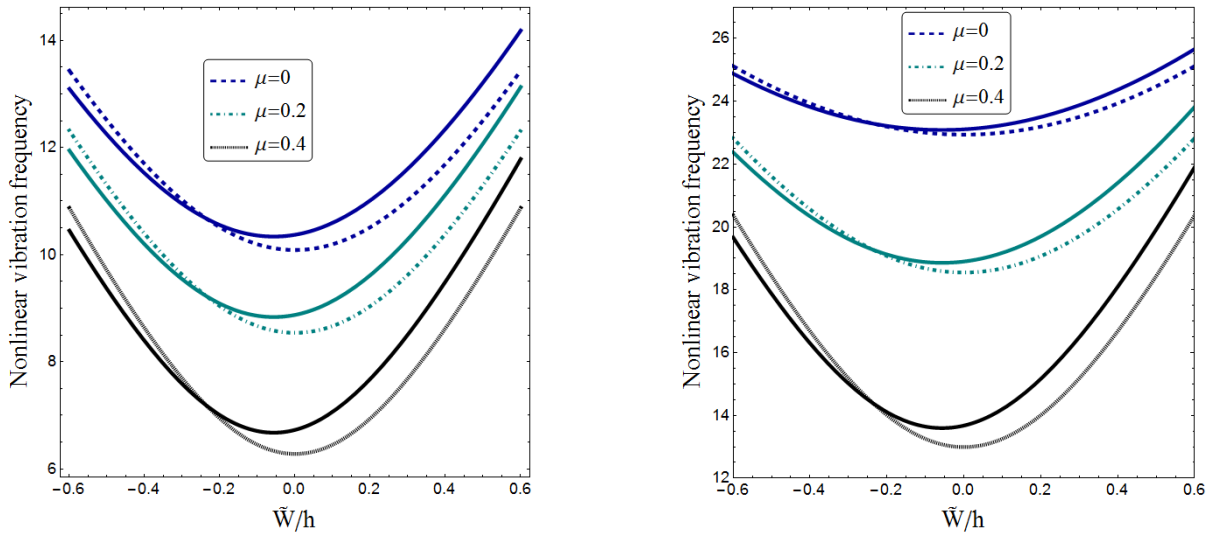

(a) S-S (b) C-C

Fig. 2 Nonlinear frequency-amplitude curves of the nanobeam for various nonlocal parameters; dashed lines: perfect nanobeam, straight lines: imperfect nanobeam (V_f = 20 %, V_E = 0, Ω = 0)

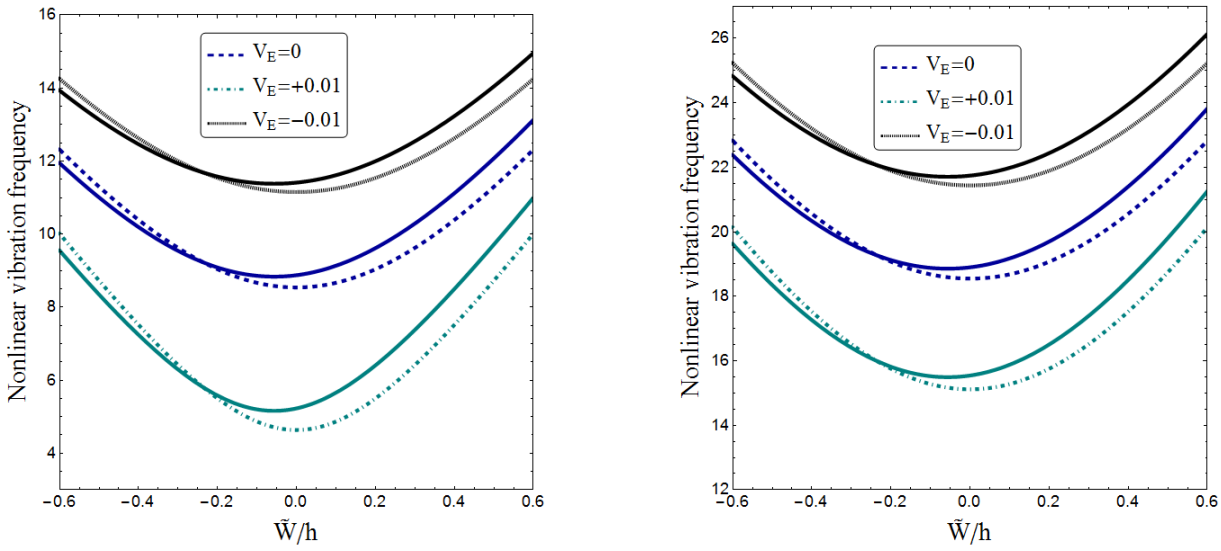

(a) S-S (b) C-C

Fig. 3 Nonlinear frequency-amplitude curves of the nanobeam for various electric voltages (V_f = 20%, μ = 0.2, Ω = 0)

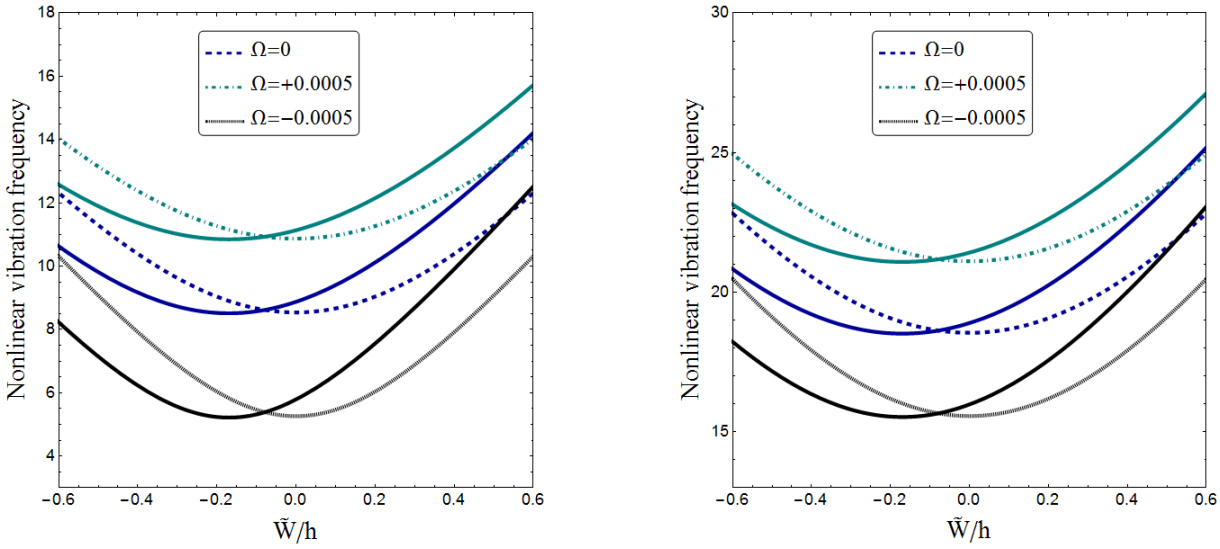

(a) S-S (b) C-C

Fig. 4 Nonlinear frequency-amplitude curves of the nanobeam for various magnetic potentials (V_f = 20%, μ = 0.2, V_E = 0)

are valid for both perfect and imperfect nano-scale beams. The new observation in this research is that when $\widetilde{W}/h < 0$, the nonlinear frequencies of an imperfect piezo-magnetic nano-scale beam diminishes at first and then increase with the rise of dimensionless amplitude, showing that there are both softening and hardening vibration behavior within a certain range of dimensionless amplitude.

Fig. 5 shows the variation of vibration frequency of a piezo-magnetic nano-scale beam versus exerted electrical voltages (VE) according to diverse values for piezoelectric constituent volume (V_f). The geometrical imperfection magnitude and dimensionless vibration amplitude are respectively considered as W*/h = 0.1 and $\widetilde{W}/h$ = 0.5. One may see that the vibration frequency stay constant by varying in electrical voltages at V_f = 0%. Thus, the nanobeam vibration is not dependent to electric voltages at zero volume of piezoelectric constituent. According to different values for Vf, varying the values of electrical voltages from negative to positive results in decrement in value of vibration frequency. The main conclusion from the figure is that the vibration frequency reduces via higher rates by increase of piezoelectric constituent volume. Thus, by increase of piezoelectric constituent volume the MEE nanobeams become more susceptible to exerted electrical voltages.

Fig. 6 depicts the effect of piezoelectric phase percentage (V_f) on the variation of vibration frequency versus applied magnetic potential. One can see from the figure that for every value of piezoelectric phase percentage, the vibration frequency increases by changing the magnetic potential from negative to positive values. As can be seen, as the piezoelectric phase percentage increases,

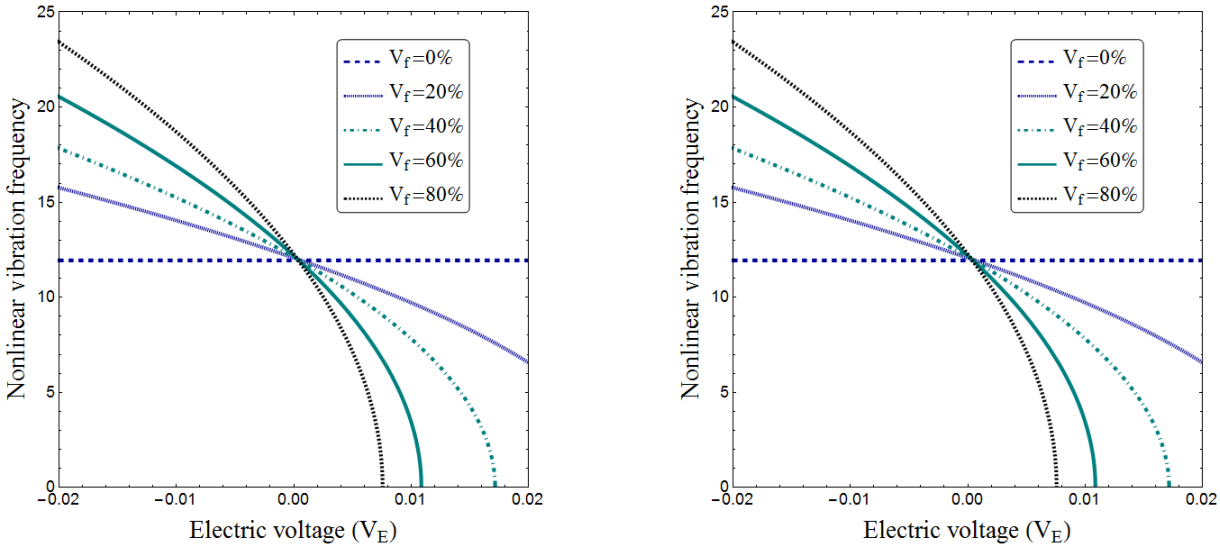

(a) S-S (b) C-C

Fig. 5 Vibration frequency of imperfect nanobeam versus electric voltage for various piezoelectric volume fractions (μ = 0.2, Ω = 0, $\widetilde{W}/h$ = 0.5, W*/h = 0.1)

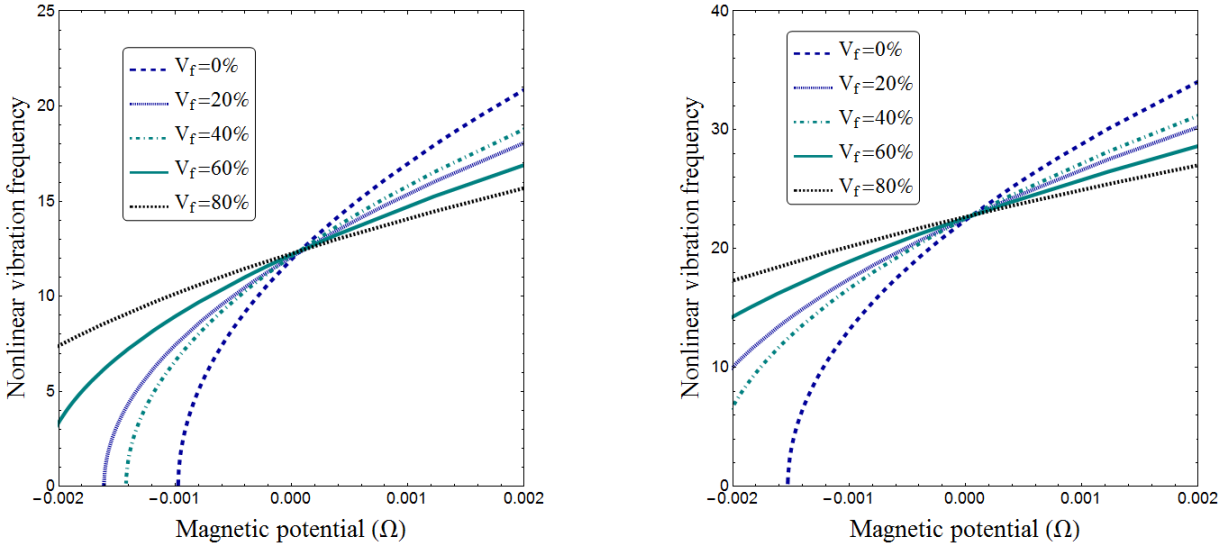

(a) S-S (b) C-C

Fig. 6 Vibration frequency of imperfect nanobeam versus magnetic potentials for various piezoelectric volume fractions (μ = 0.2, V_E = 0, $\widetilde{W}/h$ = 0.5, W*/h = 0.1)

the sensibility of vibration frequency to magnetic field reduces. So, the rate of increment in vibration frequency with respect to magnetic potential reduces with the increase of piezoelectric phase percentage. As a conclusion, for a reliable design and analysis of two-phase smart nanobeams, it is necessary to select an appropriate amount of piezoelectric phase percentage to obtain their optimum vibration behavior in magneto-electric fields.

Fig. 7 shows the effect of geometric imperfection amplitude (W*/h) on nonlinear vibration frequency of smart nanobeam having piezoelectric phase percentage of V_f = 20%. It is assumed that the nanobeam is exposed to an electric voltage of V_E = +0.01 and also a magnetic potential of Ω = 0.0005. It is seen from the figure that increasing geometric imperfection amplitude may increase the magnitude of vibration frequency. This is related to the energy stored in an imperfect nanobeam. Again, it can be observed that the nonlinear vibration characteristics of a smart nanobeam having geometrical imperfection largely depend on the vibration amplitude. In the case that $\widetilde{W}/h >$ 0, increasing magnitudes of the dimensionless amplitude can increase the nonlinear vibration frequency, highlighting the well-known "hard-spring" vibration behavior. But in the range of negative vibration amplitudes, the nonlinear vibration frequency experiences both reduction and increment.

Fig. 8 indicates the effects of linear (K_L), shear (K_P) and nonlinear (K_{NL}) springs of elastic substrate on vibration

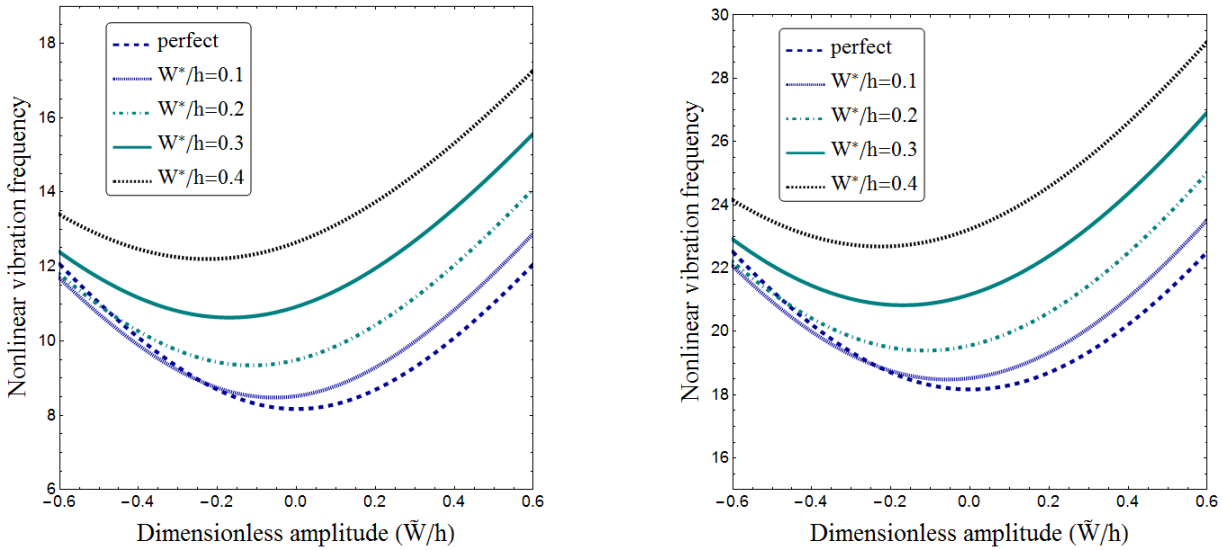

(a) S-S (b) C-C

Fig. 7 Nonlinear frequency-amplitude curves of the nanobeam for various geometric imperfections (V_f = 20%, μ = 0.2, V_E = 0.01, Ω = 0.0005)

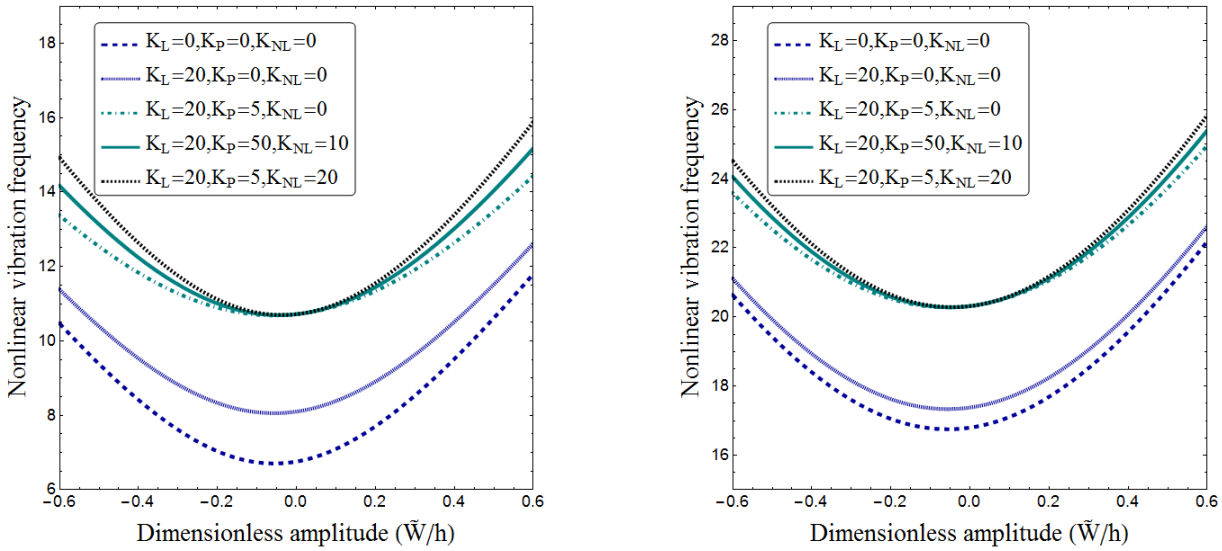

(a) S-S (b) C-C

Fig. 8 Nonlinear frequency-amplitude curves of imperfect nanobeam for various foundation parameters (V_f = 40%, μ = 0.2, V_E = 0.01, Ω = 0.0005, W*/h = 0.1)

characteristics of an imperfect smart nanobeam when the amplitude of imperfection is set to W*/h = 0.1. It is seen that increasing the magnitude of substrate coefficients makes the smart nanobeam stiffer leading to greater vibration frequencies. Also, hardening effect of the nonlinear substrate springs becomes more prominent as the magnitude of dimensionless amplitude ($\widetilde{W}/h$) increases in both positive and negative directions. But, it has no impact on vibration frequency at zero vibration amplitude. However, the influence of two other coefficients (K_L and K_P) on vibration frequency is not dependent on the magnitude of vibration amplitude.

6. Conclusions

An analysis of nonlinear free vibration behavior of smart two-phase magneto-electro-elastic nanoebeams having initial geometric imperfection was performed in this research. An analytical trend was proposed to obtain nonlinear vibration frequencies of such nanobeams for the first time.

- For both perfect and imperfect smart nanobeams, increase of nonlocal parameter let to smaller nonlinear frequencies.
- It was also seen that the nonlinear frequency of an imperfect piezo-magnetic nanobeam reduced at first

and then increased with the rise of vibration amplitude, showing that there are both softening and hardening vibration behavior within a certain range of vibration amplitude.

- By increasing in piezoelectric phase percentage the nanobeam became more sensitive to the applied electrical voltages.
- The sensitivity of vibration frequency to magnetic potential reduced with the increase of piezoelectric phase percentage.

Acknowledgement

The authors would like to thank Mustansiriyah university (www.uomustansiriyah.edu.iq) Baghdad-Iraq for its support in the present work.

References

Aboudi, J. (2001), "Micromechanical analysis of fully coupled electro-magneto-thermo-elastic multiphase composites", *Smart Mater. Struct.*, **10**(5), 867. https://doi.org/10.1088/0964-1726/10/5/303

Ahmed, R.A., Fenjan, R.M. and Faleh, N.M. (2019), "Analyzing post-buckling behavior of continuously graded FG nanobeams with geometrical imperfections", *Geomech. Eng., Int. J.*, **17**(2), 175-180. https://doi.org/10.12989/gae.2019.17.2.175

Alizada, A.N. and Sofiyev, A.H. (2011), "On the mechanics of deformation and stability of the beam with a nanocoating", *J. Reinf. Plast. Compos.*, **30**(18), 1583-1595. https://doi.org/10.1177%2F0731684411428382

Annigeri, A.R., Ganesan, N. and Swarnamani, S. (2007), "Free vibration behaviour of multiphase and layered magneto-electro-elastic beam", *J. Sound Vib.*, **299**(1-2), 44-63. https://doi.org/10.1016/j.jsv.2006.06.044

Ansari, R., Gholami, R and Rouhi, H. (2015), "Size-dependent nonlinear forced vibration analysis of magneto-electro-thermo-elastic Timoshenko nanobeams based upon the nonlocal elasticity theory", *Compos. Struct.*, **126**, 216-226. https://doi.org/10.1016/j.compstruct.2015.02.068

Arefi, M. and Zenkour, A.M. (2016), "Employing sinusoidal shear deformation plate theory for transient analysis of three layers sandwich nanoplate integrated with piezo-magnetic face-sheets", *Smart Mater. Struct.*, **25**(11), 115040. https://doi.org/10.1088/0964-1726/25/11/115040

Barati, M.R. and Zenkour, A. (2017a), "A general bi-Helmholtz nonlocal strain-gradient elasticity for wave propagation in nanoporous graded double-nanobeam systems on elastic substrate", *Compos. Struct.*, **168**, 885-892. https://doi.org/10.1016/j.compstruct.2017.02.090

Barati, M.R. and Zenkour, A.M. (2017b), "Investigating post-buckling of geometrically imperfect metal foam nanobeams with symmetric and asymmetric porosity distributions", *Compos. Struct.*, **182**, 91-98. https://doi.org/10.1016/j.compstruct.2017.09.008

Berrabah, H.M., Tounsi, A., Semmah, A. and Adda, B. (2013), "Comparison of various refined nonlocal beam theories for bending, vibration and buckling analysis of nanobeams", *Struct. Eng. Mech., Int. J.*, **48**(3), 351-365. https://doi.org/10.12989/sem.2013.48.3.351

Besseghier, A., Heireche, H., Bousahla, A.A., Tounsi, A. and Benzair, A. (2015), "Nonlinear vibration properties of a zigzag single-walled carbon nanotube embedded in a polymer matrix", *Adv. Nano Res., Int. J.*, **3**(1), 29-37. https://doi.org/10.12989/anr.2015.3.1.029

Besseghier, A., Houari, M.S.A., Tounsi, A. and Mahmoud, S.R. (2017), "Free vibration analysis of embedded nanosize FG plates using a new nonlocal trigonometric shear deformation theory", *Smart Struct. Syst., Int. J.*, **19**(6), 601-614. https://doi.org/10.12989/sss.2017.19.6.601

Bouafia, K., Kaci, A., Houari, M.S.A., Benzair, A. and Tounsi, A. (2017a), "A nonlocal quasi-3D theory for bending and free flexural vibration behaviors of functionally graded nanobeams", *Smart Struct. Syst., Int. J.*, **19**(2), 115-126. https://doi.org/10.12989/sss.2017.19.2.115

Bouafia, K., Kaci, A., Houari, M.S.A., Benzair, A. and Tounsi, A. (2017b), "A nonlocal quasi-3D theory for bending and free flexural vibration behaviors of functionally graded nanobeams", *Smart Struct. Syst., Int. J.*, **19**(2), 115-126. https://doi.org/10.12989/sss.2017.19.2.115

Bounouara, F., Benrahou, K.H., Belkorissat, I. and Tounsi, A. (2016), "A nonlocal zeroth-order shear deformation theory for free vibration of functionally graded nanoscale plates resting on elastic foundation", *Steel Compos. Struct., Int. J.*, **20**(2), 227-249. https://doi.org/10.12989/scs.2016.20.2.227

Ebrahimi, F. and Barati, M.R. (2016), "A nonlocal higher-order refined magneto-electro-viscoelastic beam model for dynamic analysis of smart nanostructures", *Int. J. Eng. Sci.*, **107**, 183-196. https://doi.org/10.1016/j.ijengsci.2016.08.001

Ebrahimi, F. and Barati, M.R. (2017), "Magnetic field effects on dynamic behavior of inhomogeneous thermo-piezo-electrically actuated nanoplates", *J. Brazil. Soc. Mech. Sci. Eng.*, **39**(6), 2203-2223. https://doi.org/10.1007/s40430-016-0646-z

Eltaher, M.A., Emam, S.A. and Mahmoud, F.F. (2012), "Free vibration analysis of functionally graded size-dependent nanobeams", *Appl. Mathe. Computat.*, **218**(14), 7406-7420. https://doi.org/10.1016/j.amc.2011.12.090

Eltaher, M.A., Khater, M.E., Park, S., Abdel-Rahman, E. and Yavuz, M. (2016), "On the static stability of nonlocal nanobeams using higher-order beam theories", *Adv. Nano. Res., Int. J.*, **4**(1), 51-64. https://doi.org/10.12989/anr.2016.4.1.051

Eringen, A.C. (1972), "Linear theory of nonlocal elasticity and vibration of curved single-walled carbon nanotubes based on nonlocal timoshenko beam theory", *Materials* dispersion of plane waves", *Int. J. Eng. Sci.*, **10**(5), 425-435. https://doi.org/10.1016/0020-7225(72)90050-X

Eshraghi, I., Jalali, S.K. and Pugno, N.M. (2016), "Imperfection sensitivity of nonlinear, **9**(9), 786. https://doi.org/10.3390/ma9090786

Guo, J., Chen, J. and Pan, E. (2016), "Static deformation of anisotropic layered magnetoelectroelastic plates based on modified couple-stress theory", *Compos. Part B: Eng.*, **107**, 84-96. https://doi.org/10.1016/j.compositesb.2016.09.044

Jandaghian, A.A. and Rahmani, O. (2016), "Free vibration analysis of magneto-electro-thermo-elastic nanobeams resting on a Pasternak foundation", *Smart Mater. Struct.*, **25**(3), 035023. https://doi.org/10.1088/0964-1726/25/3/035023

Ke, L.L. and Wang, Y.S. (2014), "Free vibration of size-dependent magneto-electro-elastic nanobeams based on the nonlocal theory", *Physica E: Low-Dimens. Syst. Nanostruct.*, **63**, 52-61. https://doi.org/10.1016/j.physe.2014.05.002

Kumaravel, A., Ganesan, N. and Sethuraman, R. (2007), "Buckling and vibration analysis of layered and multiphase magneto-electro-elastic beam under thermal environment", *Multidiscipl. Model. Mater. Struct.*, **3**(4), 461-476. https://doi.org/10.1163/157361107782106401

Li, L. and Hu, Y. (2016), "Nonlinear bending and free vibration analyses of nonlocal strain gradient beams made of functionally graded material", *Int. J. Eng. Sci.*, **107**, 77-97. https://doi.org/10.1016/j.ijengsci.2016.07.011

Li, Y. and Shi, Z. (2009), "Free vibration of a functionally graded piezoelectric beam via state-space based differential quadrature", *Compos. Struct.*, **87**(3), 257-264. https://doi.org/10.1016/j.compstruct.2008.01.012

Li, L., Tang, H. and Hu, Y. (2018), "Size-dependent nonlinear vibration of beam-type porous materials with an initial geometrical curvature", *Compos. Struct.*, **184**, 1177-1188. https://doi.org/10.1016/j.compstruct.2017.10.052

Mohammadi, H., Mahzoon, M., Mohammadi, M. and Mohammadi, M. (2014), "Postbuckling instability of nonlinear nanobeam with geometric imperfection embedded in elastic foundation", *Nonlinear Dyn.*, **76**(4), 2005-2016. https://doi.org/10.1007/s11071-014-1264-x

Mokhtar, Y., Heireche, H., Bousahla, A.A., Houari, M.S.A., Tounsi, A. and Mahmoud, S.R. (2018), "A novel shear deformation theory for buckling analysis of single layer graphene sheet based on nonlocal elasticity theory", *Smart Struct. Syst., Int. J.*, **21**(4), 397-405. https://doi.org/10.12989/sss.2018.21.4.397

Mouffoki, A., Bedia, E.A., Houari, M.S.A., Tounsi, A. and Mahmoud, S.R. (2017), "Vibration analysis of nonlocal advanced nanobeams in hygro-thermal environment using a new two-unknown trigonometric shear deformation beam theory", *Smart Struct. Syst., Int. J.*, **20**(3), 369-383. https://doi.org/10.12989/sss.2017.20.3.369

Nan, C.W. (1994), "Magnetoelectric effect in composites of piezoelectric and piezomagnetic phases", *Phys. Rev. B*, **50**(9), 6082. https://doi.org/10.1103/PhysRevB.50.6082

Pan, E. and Han, F. (2005), "Exact solution for functionally graded and layered magneto-electro-elastic plates", *Int. J. Eng. Sci.*, **43**(3-4), 321-339. https://doi.org/10.1016/j.ijengsci.2004.09.006

Shafiei, N. and She, G.L. (2018), "On vibration of functionally graded nano-tubes in the thermal environment", *Int. J. Eng. Sci.*, **133**, 84-98. https://doi.org/10.1016/j.ijengsci.2018.08.004

She, G.L., Jiang, X.Y. and Karami, B. (2019a), "On thermal snap-buckling of FG curved nanobeams", *Mater. Res. Express*, **6**, 115008. https://doi.org/10.1088/2053-1591/ab44f1

She, G.L., Ren, Y.R. and Yan, K.M. (2019b), "On snap-buckling of porous FG curved nanobeams", *Acta Astronautica*, **161**, 475-484. https://doi.org/10.1016/j.actaastro.2019.04.010

Sofiyev, A.H., Karaca, Z. and Zerin, Z. (2017), "Non-linear vibration of composite orthotropic cylindrical shells on the non-linear elastic foundations within the shear deformation theory", *Compos. Struct.*, **159**, 53-62. https://doi.org/10.1016/j.compstruct.2016.09.048

Thai, H.T. and Vo, T.P. (2012), "A nonlocal sinusoidal shear deformation beam theory with application to bending, buckling, and vibration of nanobeams", *Int. J. Eng. Sci.*, **54**, 58-66. https://doi.org/10.1016/j.ijengsci.2012.01.009

Yazid, M., Heireche, H., Tounsi, A., Bousahla, A.A. and Houari, M.S.A. (2018), "A novel nonlocal refined plate theory for stability response of orthotropic single-layer graphene sheet resting on elastic medium", *Smart Struct. Syst., Int. J.*, **21**(1), 15-25. https://doi.org/10.12989/sss.2018.21.1.015

Zemri, A., Houari, M.S.A., Bousahla, A.A. and Tounsi, A. (2015), "A mechanical response of functionally graded nanoscale beam: an assessment of a refined nonlocal shear deformation theory beam theory", *Struct. Eng. Mech., Int. J.*, **54**(4), 693-710. https://doi.org/10.12989/sem.2015.54.4.693